



Crystal structure of bis(benzylamine- κN)-[5,10,15,20-tetrakis(4-chlorophenyl)porphyrinato- $\kappa^4 N$]iron(II) *n*-hexane monosolvate

Selma Dhifaoui,^a Wafa Harhour, ^a Anna Bujacz^b and Habib Nasri^{a*}

Received 9 December 2015

Accepted 15 December 2015

Edited by M. Weil, Vienna University of Technology, Austria

Keywords: crystal structure; hydrogen bonding; UV–vis spectra; iron(II)–porphyrin; benzylamine

CCDC reference: 1442707

Supporting information: this article has supporting information at journals.iucr.org/e

^aLaboratoire de Physico-chimie des Matériaux, Faculté des Sciences de Monastir, Avenue de l'environnement, 5019 Monastir, University of Monastir, Tunisia, and ^bX-Ray Analysis Laboratory, Institute of Technical Biochemistry, Lodz University of Technology, Stefanowskiego 4/10, 90-924 Lodz, Poland. *Correspondence e-mail: hnasri1@gmail.com

In the title compound, $[\text{Fe}^{\text{II}}(\text{C}_{44}\text{H}_{24}\text{Cl}_4\text{N}_4)(\text{C}_6\text{H}_5\text{CH}_2\text{NH}_2)_2] \cdot \text{C}_6\text{H}_{14}$ or $[\text{Fe}^{\text{II}}(\text{TPP-Cl})(\text{BzNH}_2)_2] \cdot n\text{-hexane}$ [where TPP-Cl and BzNH_2 are 5,10,15,20-tetrakis(4-chlorophenyl)porphyrinate and benzylamine ligands, respectively], the Fe^{II} cation lies on an inversion centre and is octahedrally coordinated by the four pyrrole N atoms of the porphyrin ligand in the equatorial plane and by two amine N atoms of the benzylamine ligand in the axial sites. The crystal structure also contains one inversion-symmetric *n*-hexane solvent molecule per complex molecule. The average $\text{Fe}-\text{N}_{\text{pyrrole}}$ bond length [1.994 (3) Å] indicates a low-spin complex. The crystal packing is sustained by $\text{N}-\text{H} \cdots \text{Cl}$ and $\text{C}-\text{H} \cdots \text{Cl}$ hydrogen-bonding interactions and by $\text{C}-\text{H} \cdots \pi$ intermolecular interactions, leading to a three-dimensional network structure.

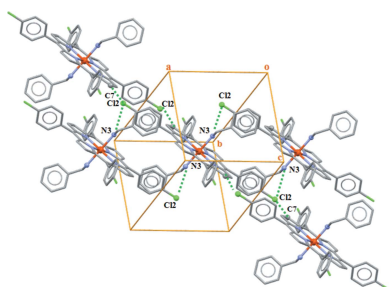
1. Chemical context

The structure of turnip cytochrome *f* has been determined on the basis of X-ray measurements (Martinez *et al.*, 1996), showing that the α -amino group of the Tyr-1 entity coordinates *trans* to the His-25 entity in the *c*-type heme protein. Thus, bis-amine Fe^{II} metalloporphyrins appear to be functionally significant as models for cytochrome *f*. On the other hand, it has been shown that the reaction of primary and secondary amines with iron(III) metalloporphyrins results in a base-catalysed one-electron reduction process and concomitant dissociation of the deprotonated amine radical (Del Gaudio & La Mar, 1978). It is also known that the addition of an excess of sterically unhindered alkylamines to an Fe(III) porphyrin derivative leads to bis(amine)–iron(II) porphyrins with the central metal cation in a six-coordination (Morice *et al.*, 1998). Notably, the number of published structures of these type of iron(II) metalloporphyrins is small. In the Cambridge Structural Database (CSD, Version 5.35; Groom & Allen, 2014), only six amine porphyrin structures are reported, including $[\text{Fe}^{\text{II}}(\text{TPP})(\text{BzNH}_2)_2]$ (TPP is the 5,10,15,20-tetraphenylporphyrinato ligand; Bz is benzyl) (Munro *et al.*, 1999).

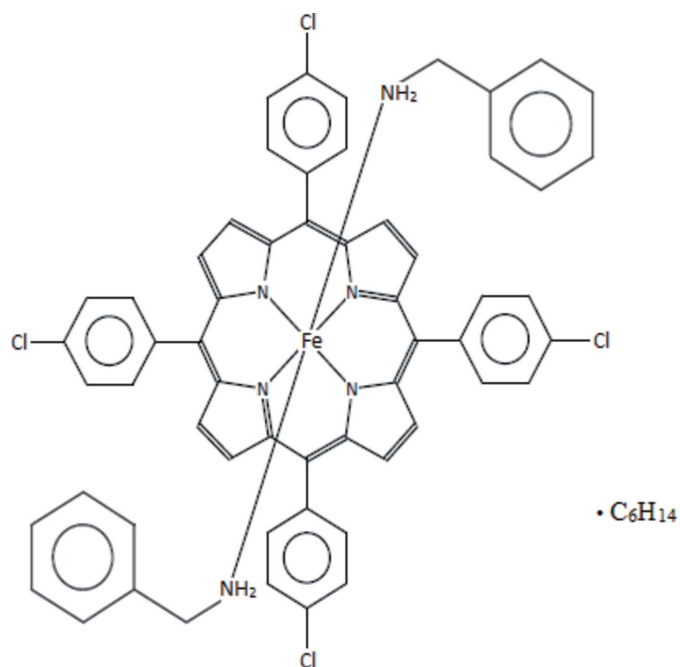
We report herein the synthesis, the molecular and crystal structures as well as UV-spectroscopic properties of bis(benzylamine)[5,10,15,20-tetra(*para*-chlorophenyl)porphyrinato]iron(II) *n*-hexane monosolvate, $[\text{Fe}^{\text{II}}(\text{TPP-Cl})(\text{BzNH}_2)_2] \cdot n\text{-hexane}$, (I).

2. Structural commentary

The molecular structure of (I) is illustrated in Fig. 1. The Fe^{II} cation is located on an inversion centre and shows an octahedral coordination environment. The equatorial plane is



formed by the four nitrogen atoms of the porphyrin moiety whereas the axial positions are occupied by the N atoms of the two benzylamine ligands.



The Fe–N_{benzylamine} bond length of 2.036 (2) Å is in the range of other iron(II)–bis(amine) porphyrin complexes [1.799–2.285 Å] reported in the literature (CSD refcodes FAVGUE: Godbout *et al.*, 1999; IMELIV: Wyllie *et al.*, 2003) and is slightly smaller than in the related structure of [Fe^{II}(TPP)(BzNH₂)₂] [2.043 (3) Å; Munro *et al.*, 1999]. The

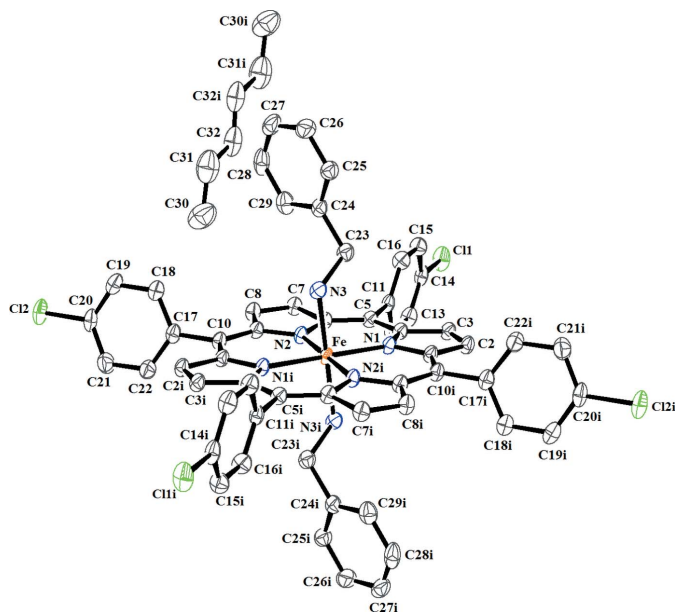


Figure 1

The structures of the molecular entities in the title compound. Displacement ellipsoids are drawn at the 60% probability level. H atoms have been omitted for clarity. [Symmetry code: (i) $-x + 1, -y + 1, -z + 1$.]

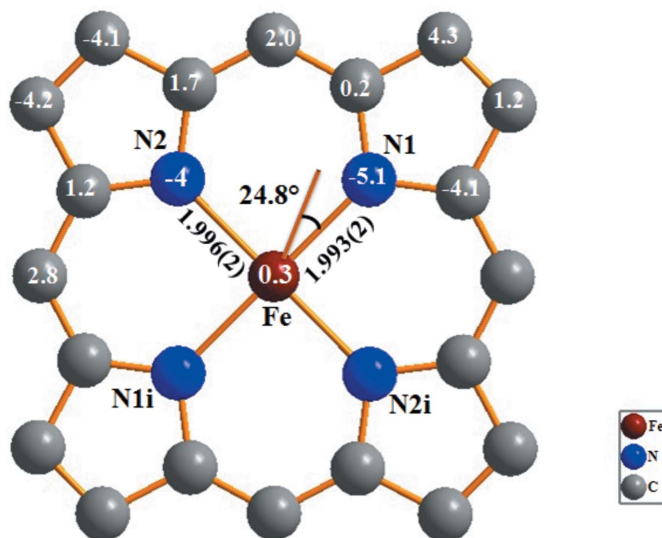


Figure 2

Schematic representation of the porphyrin core illustrating the displacements of each atom from the 24-atom plane in units of 0.01 Å.

porphyrin core of (I) is represented in Fig. 2. The porphyrin macrocycle presents a nearly planar conformation with maximum and minimum deviations from the C₂₀N₄ least-squares plane of 0.044 (2) and -0.051 (2) Å for atoms C3 and N1, respectively, while the Fe^{II} cation is co-planar with this plane with a minute deviation of 0.003 (1) Å. The α -CH₂ group of the benzylamine ligand is inclined at 24.8 (1)° relative to the shortest Fe–N_{pyrrole} bond (Fe–N1). This value is close to those of the related [Fe^{II}(TPP)(BzNH₂)₂] derivative [18.2 (4), 30.1 (4)°; Munro *et al.*, 1999].

For iron(II) porphyrins, the relationship between the spin-state of the Fe^{II} cation and the value of the average equatorial Fe–N_{pyrrole} bond length has been discussed (Scheidt & Reed, 1981). For high-spin ($S = 2$) complexes, the Fe–N_{pyrrole} bond lengths are the longest, *e.g.* for the [Fe(TpivPP)(NO₃)[−]] complex (TpivPP = picket-fence porphyrin), Fe–N_{pyrrole} amounts to 2.070 (16) Å (Nasri *et al.*, 2006). For low-spin ($S = 0$) complexes, the average Fe–N_{pyrrole} bond length is shorter, *e.g.* for the [Fe(TPP)(4-MePip)₂] complex (4-MePip is 4-methyl piperidine), the Fe–N_{pyrrole} bond length is 1.994 (4) Å (Munro & Ntshangase, 2003) and 1.990 (15) Å for the [Fe^{II}(TpivPP)(NO₂)(pyridine)][−] species (Nasri *et al.*, 2000). The intermediate spin state ($S = 1$) of Fe^{II} porphyrin complexes is represented by the shortest Fe–N_{pyrrole} distances, *e.g.* Fe(TTP) exhibits an Fe–N_{pyrrole} bond length of 1.979 (6) Å (Hu *et al.*, 2007). The averaged Fe–N_{pyrrole} bond length of 1.994 (3) Å for (I) is an indication that this species has a low-spin state ($S = 0$). This value is virtually the same as in the related [Fe^{II}(TPP)(BzNH₂)₂] derivative [Fe–N_{pyrrole} = 1.992 (4) Å; Munro *et al.*, 1999].

3. Supramolecular features

The complex molecules are packed in such a way that channels are formed parallel to [010] in which the *n*-hexane molecules

Table 1

Hydrogen-bond geometry (Å, °).

Cg1 and Cg7 are the centroids of the N1/C1–C4 and C11–C16 rings, respectively.

$D-H\cdots A$	$D-H$	$H\cdots A$	$D\cdots A$	$D-H\cdots A$
C19–H19 \cdots Cg1 ⁱ	0.93	2.66	3.586 (3)	133
C31–H31A \cdots Cg7 ⁱ	0.97	2.63	3.701 (5)	160
N3–H3B \cdots Cl2 ⁱⁱ	0.89	2.68	3.651 (2)	133
C7–H7 \cdots Cl2 ⁱⁱⁱ	0.93	3.00	3.926 (2)	175

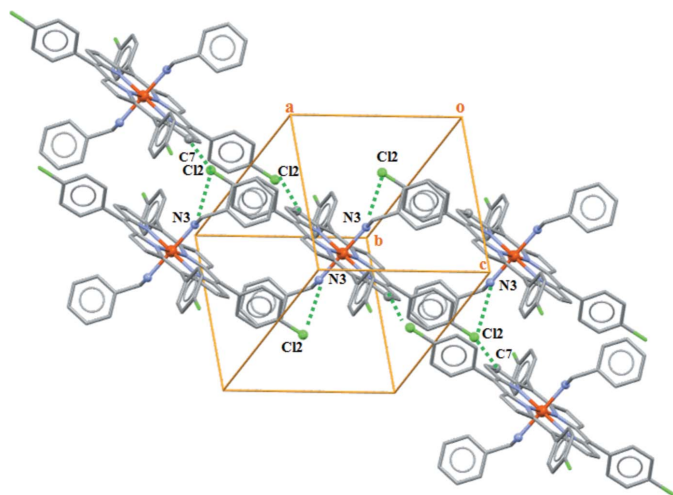
 Symmetry codes: (i) $x - 1, y, z$; (ii) $-x, -y + 1, -z + 1$; (iii) $-x, -y + 1, -z + 2$.

are situated. The linkage of the molecular components in the crystal structure of (I) is accomplished by C–H \cdots Cl, N–H \cdots Cl hydrogen-bonding interactions as well as C–H \cdots π interactions (Figs. 3 and 4; Table 1). Each [Fe^{II}(TPP-Cl)-(BzNH₂)₂] complex is linked to neighbouring complexes through N–H \cdots Cl hydrogen bonds between the N3 atom of the benzylamine ligand and the Cl2 atom of a TPP-Cl moiety and by C–H \cdots Cl interactions between the pyrrole C7 atom and the Cl2 atom. In addition, the phenyl C19 atom of the [Fe^{II}(TCIPP)(BzNH₂)₂] complex interacts with the centroid Cg1 of the (N1/C1–C4) pyrrole ring through C–H \cdots π interactions. The three-dimensional supramolecular network is consolidated by another C–H \cdots π intramolecular interaction involving the C31 atom of the *n*-hexane solvent molecule and the centroid Cg7 of the (C11–C16) phenyl ring.

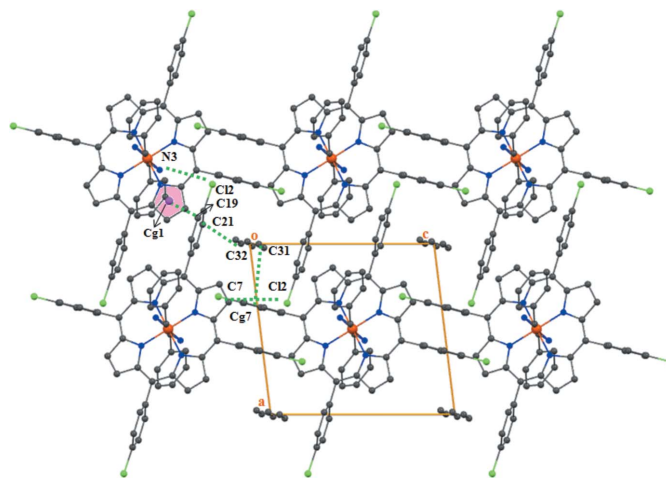
4. Synthesis

4.1. Synthesis of 5,10,15,20-tetra(*para*-chlorophenyl)porphyrin

In a 100 ml two-necked flask, 4-chlorobenzaldehyde (6 g, 42 mmol) was dissolved in 50 ml of propionic acid. The solu-


Figure 3

A partial view of the crystal packing of (I), showing the linkage between the [Fe^{II}(TPP-Cl)(BzNH₂)₂] complexes through C–H \cdots Cl and N–H \cdots Cl hydrogen bonds. The *n*-hexane solvent molecules have been omitted for clarity.


Figure 4

The crystal structure of the title compound plotted in a projection along [010]. Contacts between the entities are given as dashed lines.

tion was heated under reflux at 413 K. Freshly distilled pyrrole (3.36 ml, 42 mmol) was added dropwise and the mixture stirred for another 40 min. The mixture was then cooled overnight to 277 K and filtered *in vacuo*. The crude product was purified using column chromatography (chloroform/hexane = 4/1 *v/v* as an eluent). A purple solid was obtained that was dried *in vacuo* (1.5 g, yield 25%). UV–vis spectrum in CHCl₃: λ_{\max} ($10^{-3}\cdot\epsilon$) 420 (512.7), 516 (16.7), 552 (7.4), 591 (4.7), 646 (4.0).

4.2. Metallation of the porphyrin and synthesis of (triflato)[5,10,15,20-tetra(*para*-chlorophenyl)porphyrinato]-iron(III)

The metallation of the porphyrin was performed using the literature method to yield the chlorido–iron(III) derivative [Fe^{III}(TPP-Cl)Cl] (Collman *et al.*, 1975). We used the triflato–iron(III) TPP-Cl derivative [Fe^{III}(TPP-Cl)(SO₃CF₃)] as starting material because the triflato ligand (SO₃CF₃[−]) is much easier to substitute than the chlorido ligand. This complex was prepared according to a literature protocol (Gismelseed *et al.*, 1990).

4.3. Synthesis and crystallization of bis(benzylamine- κ N)-[5,10,15,20-tetrakis(4-chlorophenyl)porphyrinato- κ^4 N]-iron(II) *n*-hexane monosolvate complex, (I)

To a solution of [Fe^{III}(TPP-Cl)(SO₃CF₃)] (Gismelseed *et al.*, 1990) (15 mg, 0.0156 mmol) in dichloromethane (15 ml) was added an excess of benzylamine (50 mg, 0.48 mmol). The reaction mixture was stirred at room temperature for 2 h. Crystals of the title complex were obtained by diffusion of *n*-hexane through the dichloromethane solution.

5. UV–vis spectra

The UV–visible spectra with absorption bands at λ_{\max} 425/426, 532/527, 562/566 nm (CHCl₃ solution/solid state) were

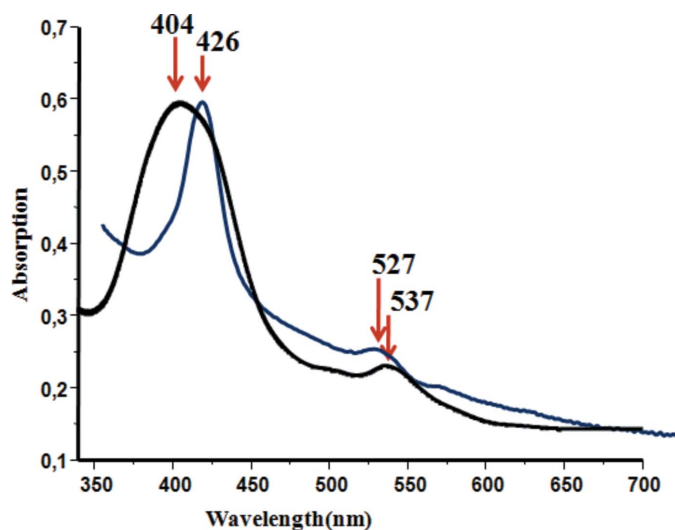


Figure 5
UV-vis spectra of the solid $[\text{Fe}^{\text{III}}(\text{TCIPP})(\text{SO}_3\text{CF}_3)]$ starting material (black) and solid (I) (blue).

recorded on a WinASPECT PLUS (validation for SPECORD PLUS version 4.2) scanning spectrophotometer. In Fig. 5 are illustrated the electronic spectra of the solid $[\text{Fe}^{\text{III}}(\text{TPP}-\text{Cl})(\text{SO}_3\text{CF}_3)]$ complex, used as starting material, and complex (I) which shows that the Soret band of the latter species is red-shifted compared to the one of the starting material. The λ_{max} values of the Soret and Q bands of (I) in the solid state and in chloroform solution are very close. These values also compare well with those of the related $[\text{Fe}^{\text{II}}(\text{TPP})(L)_2]$ ($L = 1\text{-BuNH}_2, \text{BzNH}_2, \text{PhCH}_2\text{CH}_2\text{NH}_2$) species (Munro *et al.*, 1999).

6. Refinement

Crystal data, data collection and structure refinement details are summarized in Table 2. H atoms were positioned geometrically and refined using a riding model with $\text{C}-\text{H} = 0.93 \text{ \AA}$ (aromatic), 0.97 \AA (methylene), 0.96 \AA (methyl) and $\text{N}-\text{H} = 0.89 \text{ \AA}$ for the axial ligand, with $U_{\text{iso}}(\text{H}_{\text{phenyl}}), U_{\text{iso}}(\text{H}_{\text{methylene}}), U_{\text{iso}}(\text{H}_{\text{amine}}) = 1.2U_{\text{eq}}(\text{C}/\text{N})$ and $U_{\text{iso}}(\text{H}_{\text{methyl}}) = 1.5U_{\text{eq}}(\text{C})$.

Acknowledgements

The authors gratefully acknowledge financial support from the Ministry of Higher Education and Scientific Research of Tunisia.

References

- Agilent (2014). *CrysAlis PRO*. Agilent Technologies UK Ltd, Yarnton, England.
- Burla, M. C., Caliandro, R., Camalli, M., Carrozzini, B., Cascarano, G. L., De Caro, L., Giacovazzo, C., Polidori, G. & Spagna, R. (2005). *J. Appl. Cryst.* **38**, 381–388.
- Burnett, M. N. & Johnson, C. K. (1996). *ORTEP-III*. Report ORNL-6895. Oak Ridge National Laboratory, Tennessee, USA.
- Collman, J. P., Gagne, R. R., Reed, C. A., Halbert, T. R., Lang, G. & Robinson, W. T. (1975). *J. Am. Chem. Soc.* **97**, 1427–1439.

Table 2

Experimental details.

Crystal data	
Chemical formula	$[\text{Fe}(\text{C}_{44}\text{H}_{24}\text{Cl}_4\text{N}_4)(\text{C}_7\text{H}_9\text{N})_2] \cdot \text{C}_6\text{H}_{14}$
M_r	1106.79
Crystal system, space group	Triclinic, $P\bar{1}$
Temperature (K)	100
a, b, c (Å)	10.7986 (6), 11.0555 (6), 11.4118 (4)
α, β, γ (°)	87.918 (4), 82.785 (4), 79.815 (5)
V (Å ³)	1330.16 (12)
Z	1
Radiation type	Cu $K\alpha$
μ (mm ⁻¹)	4.50
Crystal size (mm)	$0.4 \times 0.3 \times 0.1$
Data collection	
Diffractometer	Agilent SuperNova Dual Source diffractometer with a TitanS2 detector
Absorption correction	Multi-scan (<i>CrysAlis PRO</i> ; Agilent, 2014)
$T_{\text{min}}, T_{\text{max}}$	0.416, 1.000
No. of measured, independent and observed [$I > 2\sigma(I)$] reflections	12765, 5355, 4825
R_{int}	0.028
$(\sin \theta/\lambda)_{\text{max}}$ (Å ⁻¹)	0.627
Refinement	
$R[F^2 > 2\sigma(F^2)], wR(F^2), S$	0.048, 0.133, 1.06
No. of reflections	5355
No. of parameters	340
H-atom treatment	H-atom parameters constrained
$\Delta\rho_{\text{max}}, \Delta\rho_{\text{min}}$ (e Å ⁻³)	1.09, -0.54

Computer programs: *CrysAlis PRO* (Agilent, 2014), *SIR2004* (Burla *et al.*, 2005), *SHELXL2014* (Sheldrick, 2015), *ORTEP-III* (Burnett & Johnson, 1996) and *ORTEP-3 for Windows and WinGX* (Farrugia, 2012).

- Del Gaudio, J. & La Mar, G. N. (1978). *J. Am. Chem. Soc.* **100**, 1112–1119.
- Farrugia, L. J. (2012). *J. Appl. Cryst.* **45**, 849–854.
- Gismelseed, A., Bominaar, E. L., Bill, E., Trautwein, A. X., Winkler, H., Nasri, H., Doppelt, P., Mandon, D., Fischer, J. & Weiss, R. (1990). *Inorg. Chem.* **29**, 2741–2749.
- Godbout, N., Sanders, L. K., Salzmann, R., Havlin, R. H., Wojdelski, M. & Oldfield, E. (1999). *J. Am. Chem. Soc.* **121**, 3829–3844.
- Groom, C. R. & Allen, F. H. (2014). *Angew. Chem. Int. Ed.* **53**, 662–671.
- Hu, C., Noll, B. C., Schulz, C. E. & Scheidt, W. R. (2007). *Inorg. Chem.* **46**, 619–621.
- Martinez, S. E., Huang, D., Ponomarev, M., Cramer, W. A. & Smith, J. L. (1996). *Protein Sci.* **5**, 1081–1092.
- Morice, C., Le Maux, P. & Simonneaux, G. (1998). *Inorg. Chem.* **37**, 6100–6103.
- Munro, O. Q., Madlala, P. S., Warby, R. A. F., Seda, T. B. & Hearne, G. (1999). *Inorg. Chem.* **38**, 4724–4736.
- Munro, O. Q. & Ntshangase, M. M. (2003). *Acta Cryst.* **C59**, m224–m227.
- Nasri, H., Ellison, M. K., Krebs, C., Huynh, B. H. & Scheidt, W. R. (2000). *J. Am. Chem. Soc.* **122**, 10795–10804.
- Nasri, H., Ellison, M. K., Shaevitz, B., Gupta, G. P. & Scheidt, W. R. (2006). *J. Am. Chem. Soc.* **128**, 5284–5290.
- Scheidt, W. R. & Reed, C. A. (1981). *J. Am. Chem. Soc.* **103**, 543–555.
- Sheldrick, G. M. (2015). *Acta Cryst.* **C71**, 3–8.
- Wyllie, G. R. A., Schulz, C. E. & Scheidt, W. R. J. (2003). *Inorg. Chem.* **42**, 5722–5734.

supporting information

Acta Cryst. (2016). E72, 102-105 [doi:10.1107/S2056989015024135]

Crystal structure of bis(benzylamine- κ N)[5,10,15,20-tetrakis(4-chlorophenyl)-porphyrinato- κ^4 N]iron(II) *n*-hexane monosolvate

Selma Dhifaoui, Wafa Harhour, Anna Bujacz and Habib Nasri

Computing details

Data collection: *CrysAlis PRO* (Agilent, 2014); cell refinement: *CrysAlis PRO* (Agilent, 2014); data reduction: *CrysAlis PRO* (Agilent, 2014); program(s) used to solve structure: *SIR2004* (Burla *et al.*, 2005); program(s) used to refine structure: *SHELXL2014* (Sheldrick, 2015); molecular graphics: *ORTEP-III* (Burnett & Johnson, 1996) and *ORTEP-3 for Windows* (Farrugia, 2012); software used to prepare material for publication: *WinGX* (Farrugia, 2012).

Bis(benzylamine- κ N)[5,10,15,20-tetrakis(4-chlorophenyl)porphyrinato- κ^4 N]iron(II) *n*-hexane monosolvate

Crystal data

[Fe(C₄₄H₂₄Cl₄N₄)(C₇H₉N)₂] \cdot C₆H₁₄

$M_r = 1106.79$

Triclinic, *P1*

$a = 10.7986$ (6) Å

$b = 11.0555$ (6) Å

$c = 11.4118$ (4) Å

$\alpha = 87.918$ (4)°

$\beta = 82.785$ (4)°

$\gamma = 79.815$ (5)°

$V = 1330.16$ (12) Å³

$Z = 1$

$F(000) = 576$

$D_x = 1.382$ Mg m⁻³

Cu $K\alpha$ radiation, $\lambda = 1.54184$ Å

Cell parameters from 10827 reflections

$\theta = 4.1$ – 74.9 °

$\mu = 4.50$ mm⁻¹

$T = 100$ K

Prism, dark red

$0.4 \times 0.3 \times 0.1$ mm

Data collection

Agilent SuperNova Dual Source
diffractometer with a TitanS2 detector

Radiation source: sealed X-ray tube

Detector resolution: 4.1685 pixels mm⁻¹

ω scans

Absorption correction: multi-scan

(*CrysAlis PRO*; Agilent, 2014)

$T_{\min} = 0.416$, $T_{\max} = 1.000$

12765 measured reflections

5355 independent reflections

4825 reflections with $I > 2\sigma(I)$

$R_{\text{int}} = 0.028$

$\theta_{\max} = 75.3$ °, $\theta_{\min} = 3.9$ °

$h = -13 \rightarrow 13$

$k = -13 \rightarrow 10$

$l = -14 \rightarrow 12$

Refinement

Refinement on F^2

Least-squares matrix: full

$R[F^2 > 2\sigma(F^2)] = 0.048$

$wR(F^2) = 0.133$

$S = 1.06$

5355 reflections

340 parameters

0 restraints

Hydrogen site location: inferred from
neighbouring sites

H-atom parameters constrained

$w = 1/[\sigma^2(F_o^2) + (0.0771P)^2 + 0.8782P]$

where $P = (F_o^2 + 2F_c^2)/3$

$(\Delta/\sigma)_{\max} = 0.001$

$\Delta\rho_{\max} = 1.09$ e Å⁻³

$\Delta\rho_{\min} = -0.54$ e Å⁻³

Special details

Geometry. All esds (except the esd in the dihedral angle between two l.s. planes) are estimated using the full covariance matrix. The cell esds are taken into account individually in the estimation of esds in distances, angles and torsion angles; correlations between esds in cell parameters are only used when they are defined by crystal symmetry. An approximate (isotropic) treatment of cell esds is used for estimating esds involving l.s. planes.

Fractional atomic coordinates and isotropic or equivalent isotropic displacement parameters (\AA^2)

	<i>x</i>	<i>y</i>	<i>z</i>	$U_{\text{iso}}^*/U_{\text{eq}}$
Fe	0.5000	0.5000	0.5000	0.01855 (14)
N1	0.65294 (17)	0.39615 (18)	0.55478 (16)	0.0209 (4)
N2	0.40204 (17)	0.47595 (18)	0.65683 (16)	0.0210 (4)
N3	0.43283 (18)	0.35548 (18)	0.44078 (17)	0.0238 (4)
H3A	0.3486	0.3738	0.4512	0.029*
H3B	0.4563	0.3509	0.3632	0.029*
C1	0.7729 (2)	0.3693 (2)	0.4932 (2)	0.0224 (4)
C2	0.8596 (2)	0.2991 (2)	0.5658 (2)	0.0242 (5)
H2	0.9452	0.2700	0.5437	0.029*
C3	0.7939 (2)	0.2831 (2)	0.6725 (2)	0.0242 (5)
H3	0.8255	0.2414	0.7377	0.029*
C4	0.6649 (2)	0.3434 (2)	0.6655 (2)	0.0221 (4)
C5	0.5680 (2)	0.3471 (2)	0.75867 (19)	0.0219 (4)
C6	0.4447 (2)	0.4080 (2)	0.75297 (19)	0.0226 (5)
C7	0.3420 (2)	0.4066 (2)	0.8463 (2)	0.0250 (5)
H7	0.3468	0.3666	0.9191	0.030*
C8	0.2375 (2)	0.4742 (2)	0.8080 (2)	0.0254 (5)
H8	0.1568	0.4897	0.8497	0.030*
C9	0.2745 (2)	0.5176 (2)	0.6907 (2)	0.0225 (4)
C10	0.1926 (2)	0.5909 (2)	0.6214 (2)	0.0232 (5)
C11	0.59738 (19)	0.2788 (2)	0.87045 (19)	0.0220 (5)
C12	0.6263 (2)	0.3395 (2)	0.9655 (2)	0.0269 (5)
H12	0.6267	0.4236	0.9597	0.032*
C13	0.6548 (2)	0.2760 (3)	1.0695 (2)	0.0295 (5)
H13	0.6735	0.3172	1.1329	0.035*
C14	0.6547 (2)	0.1513 (3)	1.0766 (2)	0.0281 (5)
C15	0.6267 (2)	0.0882 (2)	0.9836 (2)	0.0302 (5)
H15	0.6276	0.0039	0.9895	0.036*
C16	0.5972 (2)	0.1531 (2)	0.8810 (2)	0.0289 (5)
H16	0.5770	0.1117	0.8185	0.035*
C17	0.0571 (2)	0.6294 (2)	0.6735 (2)	0.0252 (5)
C18	-0.0257 (2)	0.5459 (3)	0.6854 (2)	0.0306 (5)
H18	0.0029	0.4657	0.6600	0.037*
C19	-0.1513 (2)	0.5807 (3)	0.7349 (2)	0.0329 (6)
H19	-0.2063	0.5242	0.7431	0.039*
C20	-0.1927 (2)	0.6994 (3)	0.7714 (2)	0.0296 (5)
C21	-0.1134 (3)	0.7858 (3)	0.7565 (3)	0.0384 (6)
H21	-0.1433	0.8668	0.7788	0.046*
C22	0.0120 (2)	0.7492 (3)	0.7077 (3)	0.0352 (6)

H22	0.0662	0.8065	0.6980	0.042*
C23	0.4696 (2)	0.2302 (2)	0.4923 (2)	0.0276 (5)
H23A	0.4913	0.2379	0.5713	0.033*
H23B	0.5444	0.1877	0.4449	0.033*
C24	0.3655 (2)	0.1546 (2)	0.4982 (2)	0.0258 (5)
C25	0.3711 (2)	0.0611 (2)	0.4198 (2)	0.0304 (5)
H25	0.4395	0.0450	0.3611	0.036*
C26	0.2759 (3)	-0.0093 (3)	0.4274 (3)	0.0397 (6)
H26	0.2810	-0.0722	0.3741	0.048*
C27	0.1738 (3)	0.0136 (3)	0.5138 (3)	0.0423 (7)
H27	0.1102	-0.0339	0.5191	0.051*
C28	0.1663 (3)	0.1070 (3)	0.5921 (3)	0.0428 (7)
H28	0.0971	0.1230	0.6500	0.051*
C29	0.2623 (3)	0.1784 (3)	0.5854 (2)	0.0347 (6)
H29	0.2570	0.2412	0.6389	0.042*
Cl1	0.69094 (6)	0.07092 (7)	1.20562 (5)	0.03984 (18)
Cl2	-0.34861 (5)	0.74242 (7)	0.83650 (5)	0.03639 (17)
C30	-0.0017 (4)	0.2924 (5)	0.9519 (4)	0.0738 (12)
H30A	-0.0290	0.3479	0.8900	0.111*
H30B	-0.0494	0.3193	1.0259	0.111*
H30C	0.0868	0.2909	0.9562	0.111*
C31	-0.0232 (4)	0.1616 (5)	0.9258 (4)	0.0739 (13)
H31A	-0.1125	0.1668	0.9185	0.089*
H31B	0.0230	0.1384	0.8492	0.089*
C32	0.0130 (3)	0.0575 (4)	1.0118 (3)	0.0581 (9)
H32A	0.1032	0.0489	1.0161	0.070*
H32B	-0.0301	0.0817	1.0893	0.070*

Atomic displacement parameters (\AA^2)

	U^{11}	U^{22}	U^{33}	U^{12}	U^{13}	U^{23}
Fe	0.0152 (2)	0.0252 (3)	0.0155 (2)	-0.00339 (18)	-0.00488 (17)	0.00556 (18)
N1	0.0167 (8)	0.0284 (10)	0.0176 (9)	-0.0040 (7)	-0.0038 (7)	0.0055 (7)
N2	0.0171 (8)	0.0276 (10)	0.0181 (9)	-0.0025 (7)	-0.0056 (7)	0.0058 (7)
N3	0.0236 (9)	0.0278 (10)	0.0217 (9)	-0.0068 (8)	-0.0083 (7)	0.0063 (7)
C1	0.0178 (10)	0.0269 (11)	0.0231 (11)	-0.0038 (8)	-0.0067 (8)	0.0056 (9)
C2	0.0174 (10)	0.0299 (12)	0.0252 (11)	-0.0028 (8)	-0.0062 (8)	0.0058 (9)
C3	0.0208 (11)	0.0291 (12)	0.0239 (11)	-0.0046 (9)	-0.0095 (8)	0.0080 (9)
C4	0.0208 (10)	0.0268 (11)	0.0198 (10)	-0.0046 (8)	-0.0075 (8)	0.0053 (8)
C5	0.0221 (10)	0.0269 (11)	0.0179 (10)	-0.0055 (8)	-0.0073 (8)	0.0055 (8)
C6	0.0228 (11)	0.0281 (12)	0.0172 (10)	-0.0046 (9)	-0.0046 (8)	0.0049 (8)
C7	0.0242 (11)	0.0316 (12)	0.0185 (10)	-0.0035 (9)	-0.0040 (8)	0.0073 (9)
C8	0.0210 (10)	0.0336 (13)	0.0200 (11)	-0.0027 (9)	-0.0010 (8)	0.0051 (9)
C9	0.0199 (10)	0.0277 (11)	0.0198 (10)	-0.0041 (8)	-0.0033 (8)	0.0041 (8)
C10	0.0178 (10)	0.0290 (12)	0.0224 (11)	-0.0029 (8)	-0.0038 (8)	0.0035 (9)
C11	0.0160 (10)	0.0312 (12)	0.0183 (10)	-0.0021 (8)	-0.0044 (8)	0.0068 (9)
C12	0.0244 (11)	0.0342 (13)	0.0220 (11)	-0.0047 (9)	-0.0051 (9)	0.0052 (9)
C13	0.0262 (11)	0.0444 (15)	0.0184 (11)	-0.0054 (10)	-0.0068 (9)	0.0037 (10)

C14	0.0177 (10)	0.0451 (14)	0.0197 (11)	-0.0021 (9)	-0.0038 (8)	0.0121 (10)
C15	0.0294 (12)	0.0327 (13)	0.0277 (12)	-0.0039 (10)	-0.0050 (10)	0.0100 (10)
C16	0.0305 (12)	0.0348 (13)	0.0224 (11)	-0.0069 (10)	-0.0072 (9)	0.0064 (10)
C17	0.0201 (11)	0.0347 (13)	0.0201 (11)	-0.0028 (9)	-0.0049 (8)	0.0087 (9)
C18	0.0225 (11)	0.0369 (14)	0.0318 (13)	-0.0038 (10)	-0.0030 (9)	0.0001 (10)
C19	0.0214 (11)	0.0459 (15)	0.0322 (13)	-0.0093 (10)	-0.0038 (10)	0.0050 (11)
C20	0.0166 (10)	0.0465 (15)	0.0229 (11)	0.0009 (10)	-0.0026 (8)	0.0079 (10)
C21	0.0279 (13)	0.0364 (15)	0.0464 (16)	0.0011 (11)	0.0021 (11)	0.0017 (12)
C22	0.0232 (12)	0.0342 (14)	0.0474 (16)	-0.0051 (10)	-0.0024 (11)	0.0060 (11)
C23	0.0253 (11)	0.0303 (12)	0.0285 (12)	-0.0045 (9)	-0.0104 (9)	0.0049 (9)
C24	0.0231 (11)	0.0284 (12)	0.0262 (11)	-0.0027 (9)	-0.0095 (9)	0.0102 (9)
C25	0.0273 (12)	0.0308 (13)	0.0336 (13)	-0.0052 (10)	-0.0072 (10)	0.0050 (10)
C26	0.0365 (14)	0.0335 (14)	0.0526 (17)	-0.0088 (11)	-0.0167 (13)	0.0054 (12)
C27	0.0281 (13)	0.0420 (16)	0.0606 (19)	-0.0124 (11)	-0.0183 (13)	0.0248 (14)
C28	0.0233 (12)	0.0570 (19)	0.0416 (15)	0.0028 (11)	-0.0005 (11)	0.0270 (14)
C29	0.0326 (13)	0.0393 (14)	0.0289 (13)	0.0012 (11)	-0.0035 (10)	0.0085 (11)
C11	0.0326 (3)	0.0590 (4)	0.0244 (3)	-0.0004 (3)	-0.0064 (2)	0.0208 (3)
C12	0.0187 (3)	0.0606 (4)	0.0256 (3)	0.0012 (2)	0.0002 (2)	0.0068 (3)
C30	0.070 (3)	0.086 (3)	0.074 (3)	-0.035 (2)	-0.018 (2)	0.021 (2)
C31	0.053 (2)	0.105 (4)	0.060 (2)	-0.003 (2)	-0.0111 (18)	0.014 (2)
C32	0.0321 (15)	0.088 (3)	0.0495 (19)	0.0010 (16)	-0.0071 (14)	0.0095 (19)

Geometric parameters (Å, °)

Fe—N1	1.9932 (18)	C15—C16	1.393 (3)
Fe—N1 ⁱ	1.9932 (18)	C15—H15	0.9300
Fe—N2	1.9955 (18)	C16—H16	0.9300
Fe—N2 ⁱ	1.9956 (18)	C17—C22	1.381 (4)
Fe—N3 ⁱ	2.036 (2)	C17—C18	1.386 (4)
Fe—N3	2.036 (2)	C18—C19	1.396 (3)
N1—C1	1.382 (3)	C18—H18	0.9300
N1—C4	1.384 (3)	C19—C20	1.371 (4)
N2—C9	1.383 (3)	C19—H19	0.9300
N2—C6	1.387 (3)	C20—C21	1.384 (4)
N3—C23	1.492 (3)	C20—C12	1.744 (2)
N3—H3A	0.8900	C21—C22	1.393 (4)
N3—H3B	0.8900	C21—H21	0.9300
C1—C10 ⁱ	1.391 (3)	C22—H22	0.9300
C1—C2	1.435 (3)	C23—C24	1.509 (3)
C2—C3	1.353 (3)	C23—H23A	0.9700
C2—H2	0.9300	C23—H23B	0.9700
C3—C4	1.444 (3)	C24—C25	1.380 (4)
C3—H3	0.9300	C24—C29	1.392 (4)
C4—C5	1.391 (3)	C25—C26	1.388 (4)
C5—C6	1.390 (3)	C25—H25	0.9300
C5—C11	1.498 (3)	C26—C27	1.377 (5)
C6—C7	1.439 (3)	C26—H26	0.9300
C7—C8	1.351 (3)	C27—C28	1.375 (5)

C7—H7	0.9300	C27—H27	0.9300
C8—C9	1.438 (3)	C28—C29	1.403 (4)
C8—H8	0.9300	C28—H28	0.9300
C9—C10	1.393 (3)	C29—H29	0.9300
C10—C1 ⁱ	1.391 (3)	C30—C31	1.550 (7)
C10—C17	1.502 (3)	C30—H30A	0.9600
C11—C16	1.391 (4)	C30—H30B	0.9600
C11—C12	1.392 (3)	C30—H30C	0.9600
C12—C13	1.396 (3)	C31—C32	1.514 (6)
C12—H12	0.9300	C31—H31A	0.9700
C13—C14	1.378 (4)	C31—H31B	0.9700
C13—H13	0.9300	C32—C32 ⁱⁱ	1.392 (9)
C14—C15	1.384 (4)	C32—H32A	0.9700
C14—C11	1.742 (2)	C32—H32B	0.9700
N1—Fe—N1 ⁱ	180.0	C15—C14—C11	119.1 (2)
N1—Fe—N2	89.69 (8)	C14—C15—C16	118.8 (2)
N1 ⁱ —Fe—N2	90.31 (8)	C14—C15—H15	120.6
N1—Fe—N2 ⁱ	90.31 (8)	C16—C15—H15	120.6
N1 ⁱ —Fe—N2 ⁱ	89.69 (8)	C11—C16—C15	121.2 (2)
N2—Fe—N2 ⁱ	180.0	C11—C16—H16	119.4
N1—Fe—N3 ⁱ	85.61 (8)	C15—C16—H16	119.4
N1 ⁱ —Fe—N3 ⁱ	94.39 (8)	C22—C17—C18	118.9 (2)
N2—Fe—N3 ⁱ	92.04 (8)	C22—C17—C10	120.6 (2)
N2 ⁱ —Fe—N3 ⁱ	87.96 (8)	C18—C17—C10	120.5 (2)
N1—Fe—N3	94.39 (8)	C17—C18—C19	120.8 (3)
N1 ⁱ —Fe—N3	85.61 (8)	C17—C18—H18	119.6
N2—Fe—N3	87.96 (8)	C19—C18—H18	119.6
N2 ⁱ —Fe—N3	92.04 (8)	C20—C19—C18	119.1 (2)
N3 ⁱ —Fe—N3	180.0	C20—C19—H19	120.4
C1—N1—C4	104.92 (18)	C18—C19—H19	120.4
C1—N1—Fe	127.30 (15)	C19—C20—C21	121.2 (2)
C4—N1—Fe	127.61 (15)	C19—C20—C12	119.3 (2)
C9—N2—C6	104.94 (18)	C21—C20—C12	119.5 (2)
C9—N2—Fe	127.24 (15)	C20—C21—C22	118.8 (3)
C6—N2—Fe	127.72 (15)	C20—C21—H21	120.6
C23—N3—Fe	119.69 (15)	C22—C21—H21	120.6
C23—N3—H3A	107.4	C17—C22—C21	121.1 (3)
Fe—N3—H3A	107.4	C17—C22—H22	119.5
C23—N3—H3B	107.4	C21—C22—H22	119.5
Fe—N3—H3B	107.4	N3—C23—C24	112.64 (19)
H3A—N3—H3B	106.9	N3—C23—H23A	109.1
N1—C1—C10 ⁱ	125.2 (2)	C24—C23—H23A	109.1
N1—C1—C2	110.57 (19)	N3—C23—H23B	109.1
C10 ⁱ —C1—C2	124.1 (2)	C24—C23—H23B	109.1
C3—C2—C1	107.4 (2)	H23A—C23—H23B	107.8
C3—C2—H2	126.3	C25—C24—C29	119.2 (2)
C1—C2—H2	126.3	C25—C24—C23	121.4 (2)

C2—C3—C4	106.6 (2)	C29—C24—C23	119.4 (2)
C2—C3—H3	126.7	C24—C25—C26	120.9 (3)
C4—C3—H3	126.7	C24—C25—H25	119.6
N1—C4—C5	125.7 (2)	C26—C25—H25	119.6
N1—C4—C3	110.55 (19)	C27—C26—C25	120.2 (3)
C5—C4—C3	123.7 (2)	C27—C26—H26	119.9
C6—C5—C4	123.7 (2)	C25—C26—H26	119.9
C6—C5—C11	118.1 (2)	C28—C27—C26	119.6 (3)
C4—C5—C11	118.13 (19)	C28—C27—H27	120.2
N2—C6—C5	125.4 (2)	C26—C27—H27	120.2
N2—C6—C7	110.37 (19)	C27—C28—C29	120.6 (3)
C5—C6—C7	124.2 (2)	C27—C28—H28	119.7
C8—C7—C6	107.1 (2)	C29—C28—H28	119.7
C8—C7—H7	126.5	C24—C29—C28	119.5 (3)
C6—C7—H7	126.5	C24—C29—H29	120.3
C7—C8—C9	107.2 (2)	C28—C29—H29	120.3
C7—C8—H8	126.4	C31—C30—H30A	109.5
C9—C8—H8	126.4	C31—C30—H30B	109.5
N2—C9—C10	125.1 (2)	H30A—C30—H30B	109.5
N2—C9—C8	110.46 (19)	C31—C30—H30C	109.5
C10—C9—C8	124.4 (2)	H30A—C30—H30C	109.5
C1 ⁱ —C10—C9	124.7 (2)	H30B—C30—H30C	109.5
C1 ⁱ —C10—C17	117.5 (2)	C32—C31—C30	119.2 (4)
C9—C10—C17	117.8 (2)	C32—C31—H31A	107.5
C16—C11—C12	118.6 (2)	C30—C31—H31A	107.5
C16—C11—C5	120.6 (2)	C32—C31—H31B	107.5
C12—C11—C5	120.8 (2)	C30—C31—H31B	107.5
C11—C12—C13	120.9 (2)	H31A—C31—H31B	107.0
C11—C12—H12	119.5	C32 ⁱⁱ —C32—C31	117.6 (4)
C13—C12—H12	119.5	C32 ⁱⁱ —C32—H32A	107.9
C14—C13—C12	119.0 (2)	C31—C32—H32A	107.9
C14—C13—H13	120.5	C32 ⁱⁱ —C32—H32B	107.9
C12—C13—H13	120.5	C31—C32—H32B	107.9
C13—C14—C15	121.5 (2)	H32A—C32—H32B	107.2
C13—C14—C11	119.4 (2)		
C4—N1—C1—C10 ⁱ	-176.9 (2)	C4—C5—C11—C16	-82.1 (3)
Fe—N1—C1—C10 ⁱ	-1.4 (3)	C6—C5—C11—C12	-84.1 (3)
C4—N1—C1—C2	0.2 (3)	C4—C5—C11—C12	97.5 (3)
Fe—N1—C1—C2	175.67 (16)	C16—C11—C12—C13	0.1 (3)
N1—C1—C2—C3	-0.3 (3)	C5—C11—C12—C13	-179.5 (2)
C10 ⁱ —C1—C2—C3	176.8 (2)	C11—C12—C13—C14	0.4 (4)
C1—C2—C3—C4	0.3 (3)	C12—C13—C14—C15	-0.3 (4)
C1—N1—C4—C5	179.8 (2)	C12—C13—C14—C11	179.66 (18)
Fe—N1—C4—C5	4.3 (3)	C13—C14—C15—C16	-0.4 (4)
C1—N1—C4—C3	0.0 (3)	C11—C14—C15—C16	179.65 (19)
Fe—N1—C4—C3	-175.45 (16)	C12—C11—C16—C15	-0.8 (4)
C2—C3—C4—N1	-0.2 (3)	C5—C11—C16—C15	178.7 (2)

C2—C3—C4—C5	-180.0 (2)	C14—C15—C16—C11	1.0 (4)
N1—C4—C5—C6	-1.6 (4)	C1 ⁱ —C10—C17—C22	-72.8 (3)
C3—C4—C5—C6	178.2 (2)	C9—C10—C17—C22	107.5 (3)
N1—C4—C5—C11	176.8 (2)	C1 ⁱ —C10—C17—C18	105.6 (3)
C3—C4—C5—C11	-3.4 (3)	C9—C10—C17—C18	-74.1 (3)
C9—N2—C6—C5	179.4 (2)	C22—C17—C18—C19	-2.3 (4)
Fe—N2—C6—C5	2.9 (3)	C10—C17—C18—C19	179.3 (2)
C9—N2—C6—C7	0.7 (3)	C17—C18—C19—C20	0.4 (4)
Fe—N2—C6—C7	-175.80 (16)	C18—C19—C20—C21	2.0 (4)
C4—C5—C6—N2	-2.2 (4)	C18—C19—C20—C12	-178.5 (2)
C11—C5—C6—N2	179.4 (2)	C19—C20—C21—C22	-2.5 (4)
C4—C5—C6—C7	176.3 (2)	C12—C20—C21—C22	178.0 (2)
C11—C5—C6—C7	-2.1 (4)	C18—C17—C22—C21	1.8 (4)
N2—C6—C7—C8	-0.6 (3)	C10—C17—C22—C21	-179.8 (2)
C5—C6—C7—C8	-179.3 (2)	C20—C21—C22—C17	0.5 (4)
C6—C7—C8—C9	0.2 (3)	Fe—N3—C23—C24	146.34 (17)
C6—N2—C9—C10	179.6 (2)	N3—C23—C24—C25	104.7 (3)
Fe—N2—C9—C10	-3.9 (4)	N3—C23—C24—C29	-76.1 (3)
C6—N2—C9—C8	-0.6 (3)	C29—C24—C25—C26	-0.4 (4)
Fe—N2—C9—C8	175.94 (16)	C23—C24—C25—C26	178.8 (2)
C7—C8—C9—N2	0.2 (3)	C24—C25—C26—C27	0.2 (4)
C7—C8—C9—C10	-179.9 (2)	C25—C26—C27—C28	0.3 (4)
N2—C9—C10—C1 ⁱ	1.4 (4)	C26—C27—C28—C29	-0.5 (4)
C8—C9—C10—C1 ⁱ	-178.4 (2)	C25—C24—C29—C28	0.1 (4)
N2—C9—C10—C17	-178.9 (2)	C23—C24—C29—C28	-179.1 (2)
C8—C9—C10—C17	1.3 (4)	C27—C28—C29—C24	0.3 (4)
C6—C5—C11—C16	96.4 (3)	C30—C31—C32—C32 ⁱⁱ	177.2 (4)

Symmetry codes: (i) $-x+1, -y+1, -z+1$; (ii) $-x, -y, -z+2$.

Hydrogen-bond geometry (\AA , $^\circ$)

*Cg*1 and *Cg*7 are the centroids of the N1/C1—C4 and C11—C16 rings, respectively.

<i>D</i> —H \cdots <i>A</i>	<i>D</i> —H	H \cdots <i>A</i>	<i>D</i> \cdots <i>A</i>	<i>D</i> —H \cdots <i>A</i>
C19—H19 \cdots <i>Cg</i> 1 ⁱⁱⁱ	0.93	2.66	3.586 (3)	133
C31—H31 <i>A</i> \cdots <i>Cg</i> 7 ⁱⁱⁱ	0.97	2.63	3.701 (5)	160
N3—H3 <i>B</i> \cdots Cl2 ^{iv}	0.89	2.68	3.651 (2)	133
C7—H7 \cdots Cl2 ^v	0.93	3.00	3.926 (2)	175

Symmetry codes: (iii) $x-1, y, z$; (iv) $-x, -y+1, -z+1$; (v) $-x, -y+1, -z+2$.